Effects of anodic oxide induced intermixing on the structural and optical properties of quantum wire structure grown on nonplanar GaAs substrate

Yong Kim,[a] Shu Yuan, R. Leon, and C. Jagadish[b]
Department of Electronic Materials Engineering, Research School of Physical Science and Engineering, Institute of Advanced Studies, The Australian National University, Canberra ACT 0200, Australia

M. Gal and M. B. Johnston
School of Physics, University of New South Wales, Sydney, NSW 2052, Australia

M. R. Phillips and M. A. Stevens Kalceff
Microstructural Analysis Unit, University of Technology, Sydney, P.O. Box 123, Broadway, NSW 2007, Australia

J. Zou and D. J. H. Cockayne
Electron Microscope Unit and Australian Key Centre for Microscopy and Microanalysis, The University of Sydney, NSW 2006, Australia

(Received 24 June 1996; accepted for publication 29 July 1996)

Effects of anodic oxide induced intermixing on the structural and optical properties of stacked GaAs quantum wire (QWR) structures grown on a sawtooth-type nonplanar GaAs substrate are investigated. Cross-sectional transmission electron microscope (XTEM) observation, temperature dependent photoluminescence (PL) and cathodoluminescence (CL) imaging were used. Intermixing was achieved by pulsed anodic oxidation of the GaAs cap layer and subsequent rapid thermal annealing, was verified by XTEM analysis. A significant enhancement of QWR PL is observed accompanied by a notable blueshift of the sidewall quantum well (SQWL) PL due to the intermixing. Furthermore, an extended necking region is observed after the intermixing by spatially resolved CL. The temperature dependence of the PL intensities of both SQWL and QWR show maxima at approximately $T \sim 110$ K indicating the role of the extended necking region in feeding carriers to SQWL and QWR. © *1996 American Institute of Physics.* [S0021-8979(96)05621-6]

I. INTRODUCTION

During the past decade, the interest in the realization of low-dimensional structures, specifically quantum wire (QWR) structures, has been growing rapidly.[1] A primary application for devices with QWR structures will be the fabrication of highly efficient laser diodes as the reduction of the dimensionality results in the alteration of the density of states (DOS) as well as formation of the additional subbands. The altered DOS modifies the differential gain profile in such a way as to enable the operation of laser diodes with reduced threshold current density and allows high speed modulation. These are ideal characteristics for signal processing.[2]

Despite expectation, based on theoretical calculations about the superior properties of the QWR structures, current technology limits the possible methods for the realization of QWR. Patterning by means of e-beam lithography and subsequent etching is the most direct way.[3] However, this technique has several drawbacks. First, due to limitation of the resolution, well defined quasi-one-dimensional subbands with large subband energy separation are not achievable. Second, the heterointerface inevitably includes a large number of process damage induced nonradiative recombination centers that reduce luminescence efficiency. Other methods that have been used to obtain QWR, are tilted superlattice growth,[4,5] strain induced confinement,[6] and cleaved edge overgrowth.[7]

Growth of QWR on nonplanar substrate shows device-accessible optical properties because of *in situ* formation of heterointerface,[8,9] in spite of fundamental problems of reproducibility and design flexibility. Furthermore, a seeded self-ordering, as Kapon *et al.* pointed out, plays a role in the formation of a crescent-shaped QWR during overgrowth on a nonplanar substrate.[10] This seeded self-ordering enables stacking of virtually identical QWR structures, which is a very important characteristic for increasing the optical gain volume. The successful operation of a QWR laser diode with stacked QWR active layers has been demonstrated.[11]

However, the areal density of QWR grown on nonplanar substrates patterned by using a contact lithography is very low. As a result, the optical gain volume of QWR is almost two orders of magnitude smaller than that for sidewall quantum wells (SQWL) covering most of the sample area. In addition, carriers generated near the surface by excitation are first diffused into SQWL and then transferred both to the QWR and to the top quantum well (QWL) before radiative recombination occurs.[12] Therefore, the transfer rate of photogenerated carriers to the QWR due to the radiative recombination in the top QWL is reduced. For these reasons, large luminescence signals of the QWR that would enable fundamental study is hard to achieve. Enhancement of photoluminescence (PL) from the QWR was found after preferential etching of the top QWL and a part of the SQWLs, since their

[a]Permanent address: Semiconductor Materials Research Center, Korea Institute of Science and Technology, P.O. Box 131, Cheongryang, Seoul, Korea.
[b]Electronic mail: cxj109@phys.anu.edu.au

 0021-8979/96/80(9)/5014/7/$10.00 © 1996 American Institute of Physics

elimination increases the transfer rate of carriers to the QWR.[13–15]

QWL intermixing has drawn a great deal of attention since the technique offers the possibility of tunning the emission wavelength, which is desirable for photonic integrated circuit applications.[16] QWR intermixing may also provide interesting opportunities for fundamental studies. First, a theoretical study predicted the possible increase in the subband energy separation after intermixing.[17] Thus, controlled intermixing can increase the energy separation between ground and excited states to a larger value than room temperature thermal energy (~26 meV). Second, preferential intermixing can be achieved since these types of QWR usually are found deeper and they are thicker than SQWL. As shown in this work, preferential intermixing can result in the luminescence enhancement of QWR.

Recently, it was demonstrated that an anodic oxide layer grown by the pulsed anodization technique can serve as a current blocking layer in laser diodes.[18] Additionally, we found that this anodic oxide layer was able to promote the intermixing of QWL after rapid thermal annealing (RTA).

In this paper, the application of this anodic oxide induced intermixing technique to the QWR structure grown on a nonplanar GaAs substrate is investigated. We believe other intermixing techniques will lead to similar results as reported in this paper.

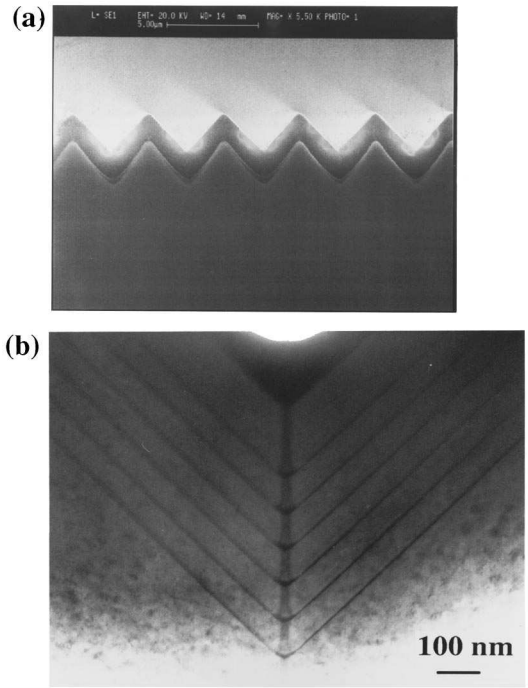

FIG. 1. (a) A scanning electron microscope image and (b) a bright-field transmission electron microscope image, both showing the stain etched cross section of the quantum wire grown on a sawtooth nonplanar substrate.

II. EXPERIMENT

Zn doped p^+ GaAs substrates were patterned using contact lithography techniques. The pattern consists of 50 2 μm-wide stripes with 2 μm spacing. After the pattern transfer, a sawtooth-type surface profile (~2.5 μm depth) is formed by wet chemical etching (H_2O:H_2O_2:H_3PO_4=3:1:1 by volume) at 0 °C. The QWR structures were grown by low pressure metalorganic chemical vapor deposition (LPMOCVD). The epitaxial layers consist of a GaAs buffer layer (~100 nm), $Al_{0.5}Ga_{0.5}As$ lower cladding layer (~1 μm), QWL active region, $Al_{0.5}Ga_{0.5}As$ upper cladding layer (~100 nm), and a GaAs capping layer (~100 nm). The active QWL region consists of 6 GaAs QWLs (~3 nm) separated by $Al_{0.5}Ga_{0.5}As$ barrier layers (~50 nm). On the bottom of the *V*-groove, six stacked QWRs are formed with the identical geometry due to the seeded self-ordering mechanism.[10] All epitaxial layers are nominally undoped and their thicknesses reported here are estimated from those obtained on planar GaAs substrate. Therefore, a slight variation of thickness is expected. The LPMOCVD system used in this study has a horizontal reactor cell with a fast switching manifold. The total flow rate of H_2 carrier gas is 17.5 slm and the operating pressure is 76 Torr. The growth temperature is 700 °C. The supply rates of trimethylgallium (TMG) and trimethylaluminum (TMA) are 2.0×10^{-5}, 3.5×10^{-5} mol/min, respectively, and the V/III ratio is 100. Planar and nonplanar substrates were loaded simultaneously and the sample grown on the planar substrate was used for calibration purpose.

The GaAs capping layer was oxidized using pulsed anodic oxidation technique. A current pulse (40 mA/cm^2 current density, 1 ms pulse width, 8.3% duty cycle) was supplied to the sample while dipping in a glycol–water–acid solution for 8 min. After the anodic oxidation, the sample was cleaved into small pieces and rapid thermal annealed in Ar ambient at 850 and 950 °C for 30 s using a proximity capping technique. GaAs substrates with a thick undoped epitaxial layer (2–4 μm) were used as supporting substrates to avoid any effects related to dopant contamination.

Cross-sectional transmission electron microscope (XTEM) specimens were prepared by ion beam thinning using a cold stage and were investigated in a Phillips EM430 electron microscope operating at 300 keV. PL was obtained using Ar^+ laser (488 nm emission wavelength) with 10 mW intensity as the excitation source, dispersed by SPEX 0.75 m spectrometer and detected by silicon photodiode. Light from an Ar^+ laser was focused on the patterned area. The beam diameter was 200 μm. The samples were cooled in a closed loop helium cryostat. Cathodoluminescence (CL) spectroscopy and spatial imaging (Oxford instrument MonoCL) of the QWR structure were carried out in a JEOL JSM35C scanning electron microscope (SEM) operated at 25 kV employing a liquid He cold stage and retractable parabolic mirror collection optics.

III. RESULTS AND DISCUSSION

Figure 1(a) shows the cross-sectional scanning electron micrograph image of an as-grown sample after stain etching indicating very regular sawtooth-type pattern. The dark layer in the SEM image corresponds to the epitaxial layer. Sidewall planes of as-etched nonplanar substrate are close to the (111)Ga plane. After growth, the sidewall planes deviate from the (111)Ga plane due to the growth rate difference between (111) and (100) planes.[19] The sawtooth nonplanar

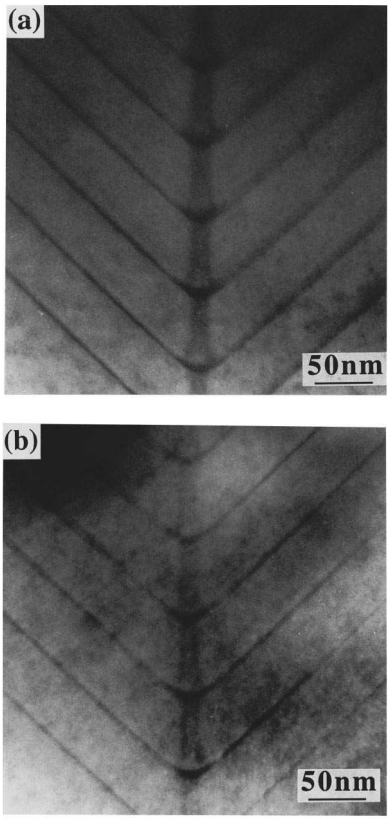

FIG. 2. Cross-sectional bright-field transmission electron microscope images of the sample as grown (a) and the sample annealed at 950 °C for 30 s with anodic oxide cap layer (b).

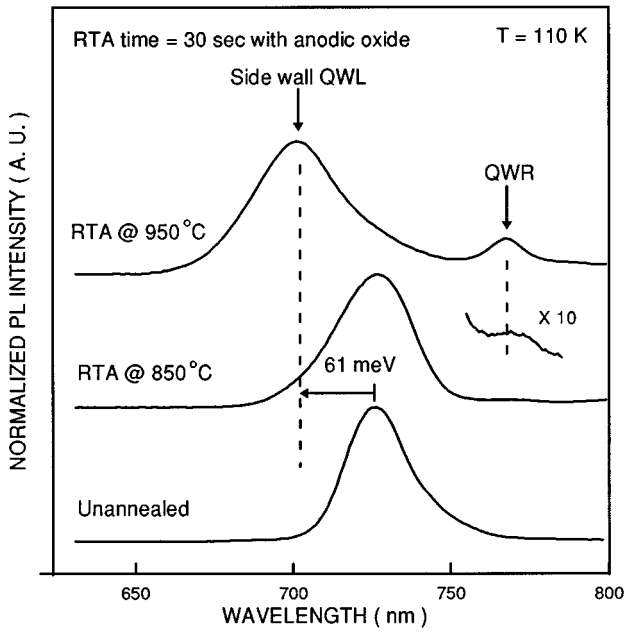

FIG. 3. Normalized photoluminescence spectra measured at 110 K for the samples annealed at 850 and 950 °C for 30 s as well as for the unannealed sample with anodic oxide cap layers.

substrate provides a minimal top QWL area after the overgrowth. Thus, the PL emission intensity from the top QWL is minimized. Figure 1(b) is a bright-field transmission electron microscopy (TEM) image, showing one of the grooves, in which six crescent shaped QWRs at the bottom of the *V* groove can be seen. Due to the mobility difference between Ga and Al species during growth, Ga species migrate preferentially toward the bottom of the *V*-groove, which offers a better nucleation site availability for Ga adatom incorporation. Thus, Ga rich vertical quantum wells (VQWL) are formed in the AlGaAs alloys at the bottom of the *V* grooves.[20] This VQWL on the TEM image appears as a vertical dark band across from the bottom of *V*-groove to the surface. VQWL plays a important role in feeding carriers to the QWR, which is very important for laser operation. As noted by Gustafsson *et al.*,[21] two branches of Ga-rich AlGaAs regions can be seen between the crescent shaped wires. Figure 2(a) shows the magnified TEM image of the sample shown in Fig. 1(b). Five QWRs from the top surface are shown in Fig. 2. The size of the fifth QWR from the surface with the most distinctive contrast was 40 nm wide and 6 nm thick. Figure 2(b) is a bright-field TEM image and shows the samples annealed at 950 °C for 30 s after anodic oxidation of the GaAs capping layer. The TEM image shows a dramatic change after RTA. First, two QWRs from the surface are intermixed and the deeper QWRs do not show any noticeable change. As can be seen in Fig. 2, a part of the VQWL near the surface is intermixed judging by the contrast difference observation to uniform AlGaAs. Furthermore, SQWLs are intermixed regardless of their depths although it is hard to draw quantitative results from the TEM analysis. The TEM analysis demonstrates SQWL intermixing while the QWR is less affected. This is presumably due to the diffusion of Ga interstitials from the anodic oxide layer into the epitaxial layer. Therefore, this process is the reverse process of the dielectric cap QWL intermixing.[16,22] In the dielectric cap QWL intermixing, Ga interstitials are considered to be dissolved into the dielectric-cap with many vacancy sites. The detailed work will be published elsewhere.

Figure 3 shows the PL spectra for the samples annealed at 850 and 950 °C as well as for the unannealed sample. All samples have oxide layers on the top surface and the measurement temperatures were kept at 110 K. No noticeable change in PL is observed for samples annealed without an oxide layer (not shown here). As shown in Fig. 1, PL is dominated by SQWL luminescence for the unannealed sample. There is no indication of emission from the QWR. After 850 °C annealing, the PL from SQWL is slightly blueshifted and weak luminescence is detected at 760 nm, which is believed to be originated from the QWR luminescence. For the sample annealed at 950 °C, SQWL luminescence is more blueshifted (~61 meV) and the QWR luminescence becomes prominent. This result supports the TEM observation of SQWL intermixing. Furthermore, the PL measurements show that the intermixing increases the transfer rate of photogenerated carriers to QWR in a similar way to the preferential etching study.[15] It is interesting to note that the PL from the SQWL shows broadening after RTA. This is due to the different intermixing rates of SQWLs depending on their depth from the surface. No noticeable blueshift of QWR luminescence was observed for the annealed samples. There-

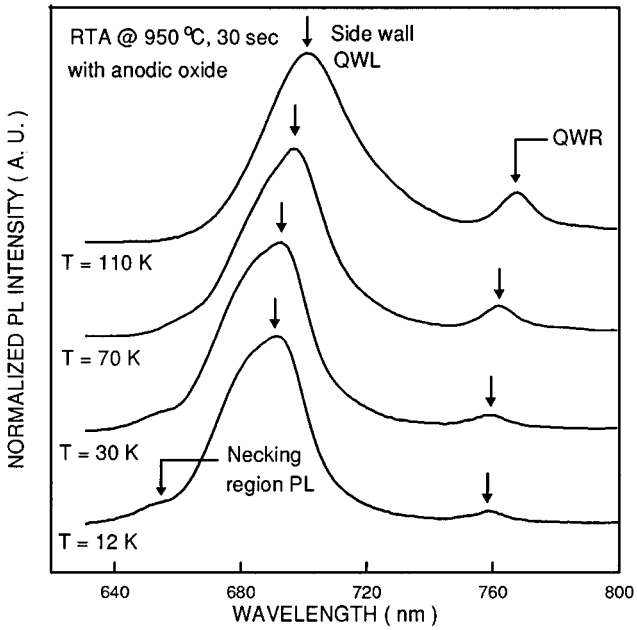

FIG. 4. Temperature dependence of the normalized photoluminescence for the quantum wire sample annealed at 950 °C for 30 s with anodic oxide cap layer.

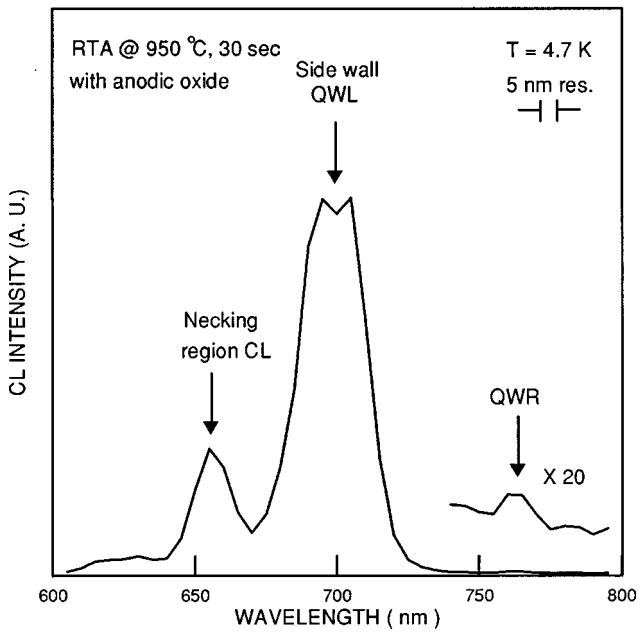

FIG. 5. Low temperature (4.7 K) cathodoluminescence spectrum for the sample annealed at 950 °C for 30 s with anodic oxide cap layer.

fore, this result shows the possibility of increasing the confinement potential by the intermixing. This increased confinement potential may result in the enhancement of subband energy splitting as discussed by Sallese *et al.*[17]

Figure 4 shows the temperature dependence of normalized PL for the sample annealed at 950 °C. As the measurement temperature increases, the relative PL intensity of QWR is increased similarly to the nonintermixed QWR luminescence.[13–15] The increase of PL of the QWR is due to the carrier thermalization in the QWR potential well. In Fig. 4, a peak (~660 nm) near the high energy tail region of the SQWL luminescence can be observed. As can be seen in Fig. 4, this peak gradually disappears as the measurement temperature increases. We attribute this peak to luminescence from the necking region. The necking region is the narrow region connecting the SQWLs and QWR, which has been assessed by high resolution XTEM.[22] In Fig. 4, the necking region PL is not resolved from the SQWL PL. The necking region PL becomes prominent and well resolved in CL spectra measured at lower temperature.

Figure 5 shows the low temperature (4.7 K) CL spectrum, for the sample annealed at 950 °C. Three distinct luminescence emissions are detected at wavelengths of 660, 700, and 760 nm. Figure 6 shows the spatially resolved CL images at these wavelengths for the identification of the luminescence origin. A secondary electron image of the structure is also displayed for comparison. The sample is tilted so that both the surface and cross section can be viewed. Accordingly, in the spatially resolved CL images, linelike and dotlike luminescence are emitted from the surface and cross section, respectively. One should distinguish the enhanced and spreaded linelike luminescences near the edge of the sample from the luminescence of the cross section even though it shows as a dotlike pattern. It is striking that the spatially resolved CL image at 660 nm [Fig. 6(b)] shows two luminescence patterns that are close to the positions of the necking region. Thus, it is considered that the 660 nm luminescence peak comes from the necking region. The separation between these two luminescence patterns and the individual pattern diameter are approximately 0.9 and 0.4 μm, respectively. To the authors' knowledge, this is the first direct observation of necking region luminescence. The 700 nm CL peak is attributed to the SQWL. The spatially resolved CL image [Fig. 6(c)] displays bright luminescence over the entire area except the QWR region. The CL at 760 nm is emitted from the QWRs that are located at the bottom of the *V* grooves as shown in Fig. 4(d). The QWR luminescence is weak at 4.7 K. However, as the measurement temperature is increased, the intensity of QWR luminescence increases gradually, as shown in Fig. 4.

Figure 7 shows the temperature dependence of PL intensities of SQWL and QWR. In the case of the nonintermixed QWR sample, the PL intensity of SQWLs is known to monotonically decrease as the measurement temperature is increased. On the other hand, the PL intensity of the QWR shows its maximum around 100 K.[13,14] This behavior was explained as resulting from the carrier transfer from SQWL to QWR. However, as shown in Fig. 7, both intensities of SQWL as well as QWR PL increase rapidly with increasing temperature at the low temperature regime and show their maximum at around 110 K. The ratios of $I^{\mathrm{SQWL(110\ K)}}/I^{\mathrm{SQWL(12\ K)}}$ and $I^{\mathrm{QWR(110)}}/I^{\mathrm{QWR(12\ K)}}$ are 2.6 and 9.1, respectively, where I^{SQWL} and I^{QWR} are PL intensities of SQWR and QWR at the measurement temperature shown in the brackets. It is noteworthy that both PL intensities show the maximum at the same temperature (~110 K). This means that carriers are transferred from the same source. One

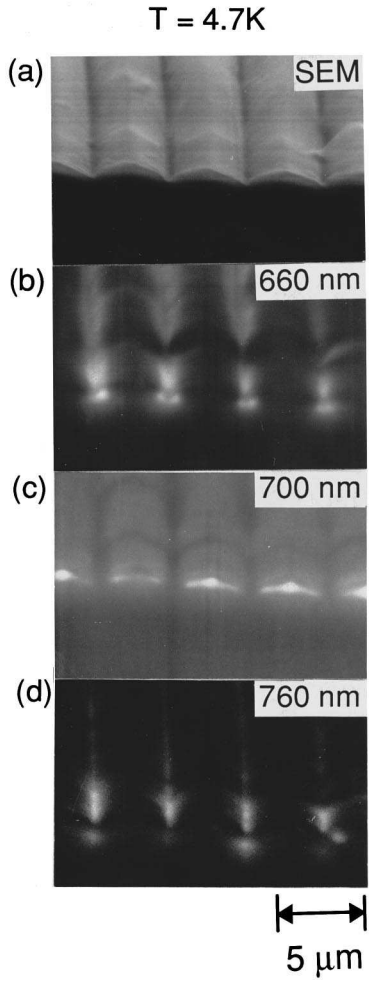

FIG. 6. Spatially resolved cathodoluminescence images (25 kV) recorded at wavelengths of 660 nm (b), 700 nm (c) and 760 nm (d). A secondary electron micrograph (a) is displayed for comparison. The sample is tilted so that the cross section and top surface are visible simultaneously. Linelike and dotlike luminescence correspond to the luminescences emitted from the top surface and cross section, respectively. Note that enhanced and spread linelike luminescences from the edge of the sample are not from the cross section.

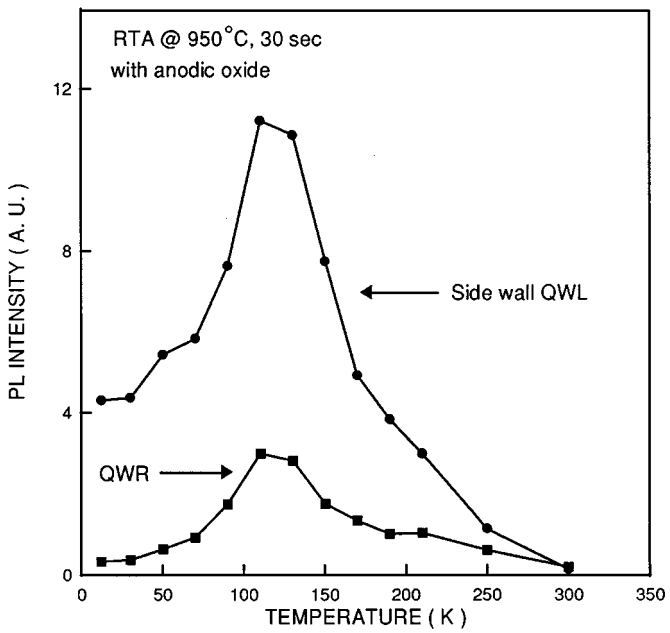

FIG. 7. Photoluminescence intensity of sidewall quantum well and quantum wire as a function of measurement temperature.

possible source is the VQWL. This possibility can be ruled out from the intermixing of VQWL observed by TEM [see Fig. 2(b)] and from the low carrier mobility of AlGaAs. Furthermore, very well defined PL intensity peaks ($T \sim 110$ K) demonstrate no hampering of optical quality after the anodic oxide induced intermixing because the carrier mobility in the GaAs/AlGaAs QWL is significantly affected by interface roughness and impurity scatterings.[23] The temperature ($T \sim 110$ K) showing the maximum intensity is consistent with the temperature of peak carrier mobility in the high quality GaAs/AlGaAs QWL with similar thickness.[24]

In the nonintermixed QWR, carriers diffuse from SQWL to QWR through the necking region.[13] The tunneling process of carriers through the energy barrier formed by the necking region explains the transfer rate.[25] Thus, there is no chance of radiative recombination during the tunneling process. However, it is not plausible that such a tunneling process occurs due to the high energy barrier of the necking region with respect to the SQWL (~108 meV) as well as the extension of the necking region. Instead, carriers generated in the AlGaAs barrier are first transferred to the extended necking region and captured both by the SQWL and the QWR. Therefore, its role is very similar to the role of the VQWL in nonintermixed QWR samples.[13]

The formation mechanism of the necking region is not understood completely. One possible explanation is the crystallographic dependence of the intermixing rate. (111) planes consist of alternating Ga and As planes. The intermixing rate on the (111) plane (i.e., SQWL) might be lower than on the (100) plane, under the same conditions, due to the tight-binding atomic configuration of the (111) plane. The *squeezing* effect by the necking region may provide another way to increase subband energy separation.[17]

Figure 8 shows the room temperature PL of the sample annealed at 950 °C for 30 s. No significant broadening of the QWR PL peak was observed presumably due to the two-dimensional confinement.[15] Furthermore, the well resolved QWR PL peak reflects no significant change in optical quality after the intermixing. Figure 9 shows the spatially resolved room temperature CL images recorded at 730 and 800 nm, respectively. Figure 9(b) displays spatially the well resolved QWR emission at room temperature. This result shows promise for the device applications of these types of QWR structures.

IV. CONCLUSION

Anodic oxide induced intermixing has been studied for QWR structures grown on nonplanar GaAs substrates. After RTA at 950 °C for 30 s with anodically oxidized GaAs capping layer, a significant PL blueshift (~61 meV) of the SQWL as well as prominent enhancement of the QWR luminescence is observed. The structural study by means of

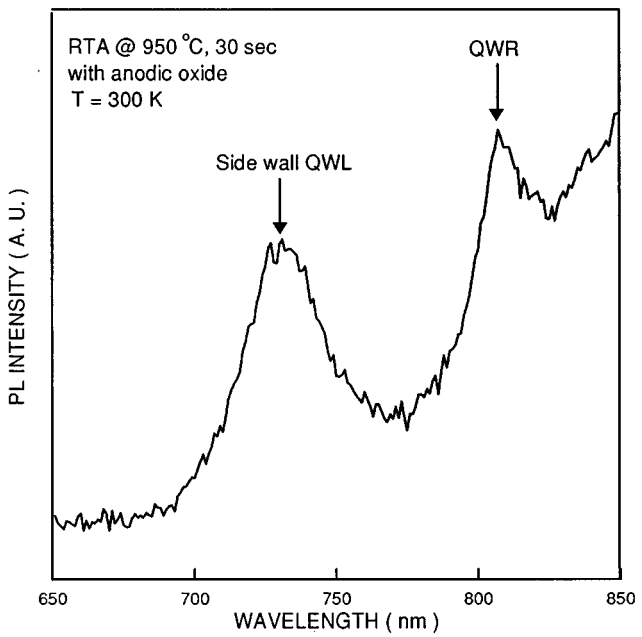

FIG. 8. Room temperature photoluminescence spectrum of the sample annealed at 950 °C for 30 s with anodic oxide cap layer.

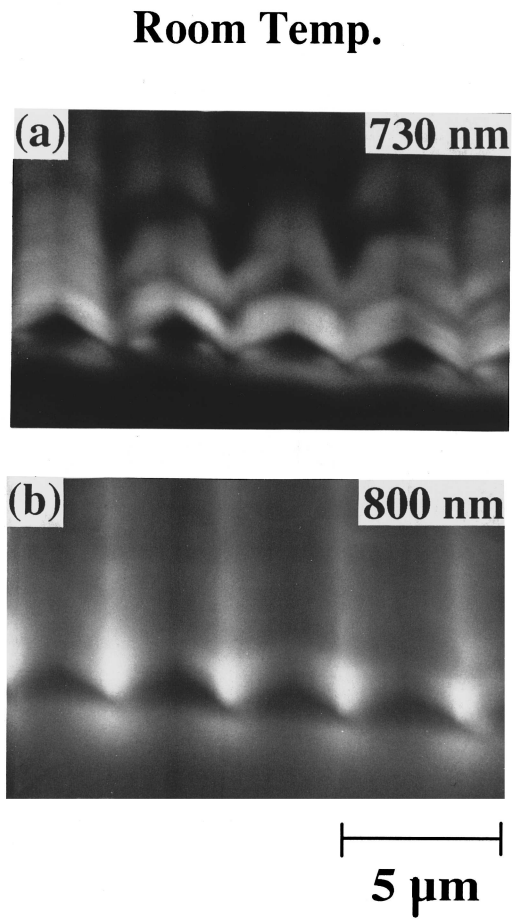

FIG. 9. Spatially resolved room temperature cathodoluminescence images (25 kV) recorded at wavelengths of 730 nm (a) and 800 nm (b) for the sample annealed at 950 °C for 30 s with anodic oxide cap layer. Note that enhanced and spread linelike luminescences from the edge of the sample are not from the cross section.

TEM shows a noticeable intermixing of the SQWLs. Spatially resolved-low temperature (4.7 K) cathodoluminescence images recorded at different wavelengths confirms the initial assignments of emissions from the SQWL and QWR. In addition, a luminescence from the necking region between SQWL and QWR is observed by CL imaging. This is attributed to the extension of the necking region by the intermixing. A temperature dependent PL study shows that the luminescence from the necking region disappears with increasing temperature. Furthermore, unlike PL from nonintermixed QWR, both SQWL and QWR show their maximum intensities at around 110 K. This is an observation that the extended necking region might have a role so that carriers generated in the AlGaAs barrier are first transferred to the extended necking region and later captured both by the SQWL and the QWR. The spatially resolved CL image and PL study at room temperature show well defined QWR luminescence, demonstrating no substantial inclusion of nonradiative recombination centers into the QWR during the intermixing.

ACKNOWLEDGMENTS

The authors are grateful to the Australian Research Council for financial support. The authors would like to thank Professor Peter Zory and Dr. Craig Largent (University of Florida) for fruitful discussions about pulsed anodic oxidation and to thank A. Sikorski for his help with TEM specimen preparation. One of the authors, Y. K., would like to thank Professor R. M. Cohen (University of Utah) for fruitful discussions about anodic oxide induced intermixing.

[1] See *Science and Engineering of 1 and 0-Dimensional Semiconductors*, edited by S. P. Beaumont and C. M. Sotomayor Torres (Plenum, New York, 1990).
[2] Y. Arakawa and A. Yariv, , IEEE J. Quantum Electron. **QE-22** 1887 (1986).
[3] H. Temkin, G. J. Dolan, M. B. Panish, and S. N. G. Chu, Appl. Phys. Lett. **50**, 413 (1987).
[4] J. M. Gaines, P. M. Petroff, H. Kroemer, R. J. Simes, R. S. Geels, and J. H. English, J. Vac. Sci. Technol. B **6**, 1378 (1988).
[5] T. Fukui and H. Saito, Appl. Phys. Lett. **50**, 824 (1987).
[6] K. Kash, R. Bhat, Derek D. Mahoney, P. S. D. Lin, A. Scherer, J. M. Worlock, B. P. Van der Gaag, M. Koza, and P. Grabbe Appl. Phys. Lett. **55**, 681 (1989).
[7] L. Pfeiffer, H. L. Stormer, K. W. Baldwin, K. W. West, A. R. Goni, A. Pinczuk, R. C. Ashoori, M. M. Dignam, and W. Wegscheider, J. Cryst. Growth **127**, 849 (1993).
[8] E. Kapon, M. Walther, J. Christen, M. Grundmann, C. Caneau, D. M. Hwang, E. Colas, R. Bhat, G. H. Song, and D. Bimberg, Superlattices Microstruct. **12**, 491 (1992).
[9] S. Tsukamoto, Y. Nagamune, N. Nishioka, and Y. Arakawa, J. Appl. Phys. **71**, 533 (1992).
[10] E. Kapon, G. Biasiol, D. M. Hwang, and E. Colas, Microelectron. J. **26**, 881 (1995).
[11] S. Simhony, E. Kapon, E. Colas, R. Bhat, N. G. Stoffel, and P. Worland, Appl. Phys. Lett. **59**, 2225 (1991).
[12] J. Christen, M. Grundmann, E. Kapon, E. Colas, D. M. Hwang, and D. Bimberg, Appl. Phys. Lett. **61**, 67 (1992).
[13] M. Walther, E. Kapon, J. Christen, D. M. Hwang, and R. Bhat, Appl. Phys. Lett. **60**, 521 (1992).
[14] Min-Suk Lee, Yong Kim, Moo-Song Kim, Seong-Il Kim, Suk-Ki Min, Young Duk Kim, and Sahn Nahm, Appl. Phys. Lett. **63**, 3052 (1993).
[15] X. L. Wang, M. Ogura, and H. Matsuhata, Appl. Phys. Lett. **67**, 3629 (1995).
[16] J. H. Marsh, Semicond. Sci. Technol. **8**, 1136 (1993).

[17] J. M. Sallese, J. F. Carlin, M. Galihanou, and P. Grunberg, Appl. Phys. Lett. **67**, 2633 (1995).
[18] M. J. Grove, D. A. Hudson, P. S. Zory, R. J. Dalby, C. M. Harding, and A. Rosenberg, J. Appl. Phys. **76**, 587 (1994).
[19] S. D. Hersee, E. Barbier, and R. Blondeau, J. Cryst. Growth **77**, 310 (1986).
[20] G. Vermeire, Z. Q. Yu, F. Vermaerke, L. Buydens, P. Van Daele, and P. Demeester, J. Cryst. Growth **124**, 513 (1992).
[21] A. Gustafsson, F. Reinhardt, G. Biasiol, and E. Kapon, Appl. Phys. Lett. **67**, 3673 (1995).
[22] W. J. Choi, S. Lee, Y. Kim, D. Woo, S. K. Kim, S. H. Kim, J. I. Lee, K. N. Kang, J. H. Chu, S. K. Yu, J. C. Seo, D. Kim, and K. Cho, Appl. Phys. Lett. **67**, 3438 (1995).
[23] H. Hilmer, A. Forchel, R. Sauer, and C. W. Tu, Phys. Rev. B **42**, 3220 (1990).
[24] H. Hilmer, A. Forchel, S. Hansmann, M. Morohashi, E. Lopez, H. P. Meirer, and K. Ploog, Phys. Rev. B **39**, 10 901 (1989).
[25] Yong Zhang, M. D. Sturge, K. Kash, B. P. van der Gaag, A. S. Gozdz, L. T. Florez, and J. P. Harbison, Phys. Rev. B **51**, 13 303 (1995).